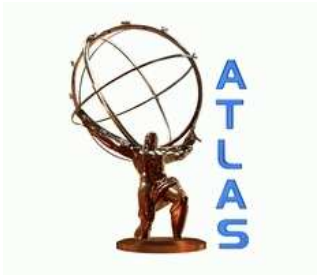

ATLAS NOTE

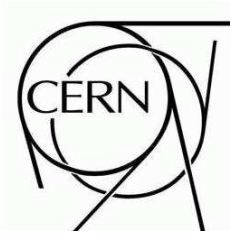

Multi-Lepton Supersymmetry Searches

The ATLAS Collaboration[1)]

This note is part of CERN-OPEN-2008-020. This version of the note should not be cited: all citations should be to CERN-OPEN-2008-020.

ATL-PHYS-PUB-2009-068
10 May 2009

Abstract

We investigate the potential of the ATLAS detector to discover new physics events containing three leptons and missing transverse momentum. Such final states are predicted in a variety of extensions to the Standard Model. In the context of supersymmetric models, they could result from direct production of gaugino pairs. Using Monte Carlo simulations we present the discovery potential for several benchmark Supersymmetry points. We pay particular attention to the case where all strongly interacting sparticles are heavy. We investigate trigger and reconstruction efficiencies and discuss methods for measuring various systematic uncertainties. A solid discovery is expected with an integrated luminosity of the order of several inverse fb. If coloured particles are heavy direct production of gauginos dominates. In such scenarios, discovery would require about an order of magnitude larger luminosity.

[1)]This note prepared by A.J. Barr, O.E. Brandt, P. Bruckman de Renstrom, A. De Santo, J. Dragic, K. Pajchel, C. Potter, T. Sarangi and C. Serfon.

1 Introduction

If supersymmetric (or other partner) particle production at the LHC is dominated by particles without colour charge, then one of the most promising discovery channels is in multi-lepton + missing transverse momentum ($E_{\mathrm{T}}^{\mathrm{miss}}$) final states with little hadronic activity. In this section we investigate the ability of the ATLAS experiment to discover new physics in events containing three (or more) leptons – either electrons or muons – of which two must have opposite signs but the same flavour (OSSF). We determine the sensitivity which would be obtained for discovery of five benchmark points with an integrated luminosity of 10 fb^{-1}.

While an analysis of this channel is clearly sensitive to other models, in this section we use Supersymmetry as our example signature, we assume R-parity conservation, and that the lightest SUSY particle (LSP) is the weakly interacting $\tilde{\chi}_1^0$, which provides the missing transverse energy signal.

In the supersymmetric case, the final states of interest could come from leptonic decay of pairs of heavy gauginos (such as $\tilde{\chi}_2^0$ and $\tilde{\chi}_1^+$) through real or virtual $W^{\pm}$, Z^0 or sleptons to leptons and a pair of LSPs. The heavy gauginos may be produced directly, or in the decay of heavier partner particles.

The primary aim is to make the most realistic determination which is possible at this time of the discovery potential in this channel. We also wish to identify the most important Standard Model backgrounds, so that analyses can be prepared to measure them in control regions with the ATLAS data.

Throughout this study we use the inclusive Supersymmetry production Monte Carlo samples described in [1]. The points lie in various regions of mSUGRA parameter space in which the LSP relic density is broadly consistent with the observed cold dark matter density.

The Standard Model backgrounds simulated are listed in Table 1. The most important backgrounds are found to be $t\bar{t}$, Zb and ZW. Fully leptonic ZW events represent one significant source of events containing three leptons and missing energy. Their contribution can be reduced by rejecting OSSF lepton pairs with invariant masses consistent with the Z mass. Leptonic decays of $t\bar{t}$, and Zb are expected to produce two leptons but can generate a third from leptonic b quark decay. These backgrounds have large cross-sections, but can be reduced by the introduction of stringent cuts on the isolation of the lepton tracks – as we will discuss in Section 3.

Table 1: List of the background samples used, with Monte Carlo generator cross-sections (σ), next-to-leading-order to leading-order k factors (where known for leading-order generators), average weights ($\langle \mathrm{w} \rangle$) and corresponding integrated luminosities. The cross-sections for WW, WZ, ZZ, $Z\gamma$ and Zb are quoted after a filter is applied on the generator output requiring at least one lepton with pseudorapidity, $|\eta| < 2.8$ and transverse momentum, $p_T > 10$ GeV. The diboson (WW, WZ, ZZ) samples have a different cross-section than the diboson MC@NLO samples (found elsewhere in this volume) because they also include contributions from (and interference with) the photon pole.

Process	σ [pb]	k factor	$\langle \mathrm{w} \rangle$	$\int \mathrm{d}t\,\mathscr{L}$ [fb^{-1}]
WW	24.5	1.67	1	1.22
WZ	7.8	2.05	1	2.98
ZZ	2.1	1.88	1	12.7
$Z\gamma$	2.6	1.30	1	2.98
Zb	154	1	0.66	0.75
$t\bar{t}$	450	-	0.73	0.92

A particularly important benchmark point for the trilepton analysis is the point SU2 [1]. This point lies within the 'focus point' region of mSUGRA parameter space which is characterised by very large masses for squarks and sleptons and relatively light gauginos. The heavy squarks and sleptons (see Figure 1 and Table 2 for the SUSY mass hierarchy at SU2), will have very small production cross-sections at the LHC and make it a difficult region in which to discover SUSY using the analyses described in [2]

based on the selection of hadronic jets and missing transverse momentum [3]. However, gaugino and gluino production will still be abundant, so we expect good discovery potential in multi-lepton events. The branching ratios of gauginos for SU2 can be found in Table 3[2)].

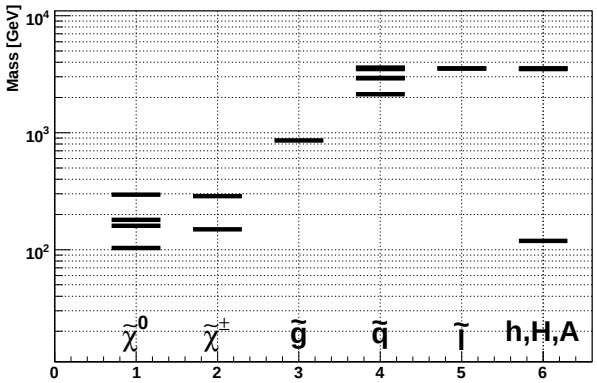

Figure 1: SU2 sparticle mass spectrum.

Table 2: Particle masses for SU2.

Sparticle	Mass [GeV]	Sparticle	Mass [GeV]
$\tilde{\chi}_1^0$	103	$\tilde{g}$	857
$\tilde{\chi}_2^0$	160	$\tilde{u}_L$	3563
$\tilde{\chi}_3^0$	180	$\tilde{u}_R$	3574
$\tilde{\chi}_4^0$	295	$\tilde{d}_L$	3564
$\tilde{\chi}_1^\pm$	149	$\tilde{d}_R$	3576
$\tilde{\chi}_2^\pm$	287	$\tilde{b}_1$	2925
$\tilde{\ell}_L$	3548	$\tilde{b}_2$	3501
$\tilde{\ell}_R$	3547	$\tilde{t}_1$	2131
$\tilde{\nu}_L$	3546	$\tilde{t}_2$	2935

The total cross-section times branching ratio for chargino-neutralino direct pair production and decay to a trilepton final state is 32.6 fb. Table 4 shows the contribution from each $\tilde{\chi}^\pm\ \tilde{\chi}^0$ pair production to a trilepton final state. The contribution from $\tilde{\chi}^\pm\ \tilde{\chi}^\mp$ and $\tilde{\chi}^0\ \tilde{\chi}^0$ pair production to a trilepton final state is not tabulated, but also adds a small contribution to the signal. Exclusive trilepton signal for SU2 is dominated by the pair production $\tilde{\chi}_1^\pm\ \tilde{\chi}_2^0$ followed by $\tilde{\chi}_1^\pm \rightarrow \tilde{\chi}_1^0\ \ell\nu$ and $\tilde{\chi}_2^0 \rightarrow \tilde{\chi}_1^0\ \ell^+\ell^-$ decays.

Table 3: Some important branching ratios for the benchmark point SU2.

Sparticle	Decay Mode	B.R.
$\tilde{\chi}_2^0$	$\tilde{\chi}_1^0\ell^+\ell^-$	7%
$\tilde{\chi}_3^0$	$\tilde{\chi}_1^0\ell^+\ell^-$	7%
$\tilde{\chi}_4^0$	$\tilde{\chi}_1^\pm W^\mp$	81%
	$\tilde{\chi}_3^0 Z$	12%
$\tilde{\chi}_1^\pm$	$\tilde{\chi}_1^0\ell\nu$	22%
$\tilde{\chi}_2^\pm$	$\tilde{\chi}_2^0 W^\pm$	38%
	$\tilde{\chi}_3^0 W^\pm$	18%
	$\tilde{\chi}_1^\pm Z$	30%

Table 4: Leading-order cross-sections and number of trilepton events for integrated luminosity of 10 fb^{-1} for SU2.

Production	σ [fb]	Trilepton events /10 fb^{-1}
$\tilde{\chi}_1^\pm\tilde{\chi}_2^0$	1138.0	175
$\tilde{\chi}_1^\pm\tilde{\chi}_3^0$	679.3	105
$\tilde{\chi}_1^\pm\tilde{\chi}_4^0$	51.4	6
$\tilde{\chi}_2^\pm\tilde{\chi}_2^0$	58.5	7
$\tilde{\chi}_2^\pm\tilde{\chi}_3^0$	61.6	7
$\tilde{\chi}_2^\pm\tilde{\chi}_4^0$	310.3	26
TOTAL		326

The trilepton signal may include contributions both from direct gaugino pair events and from other SUSY events. The latter can lead to trilepton final states when cascades initiated by heavier sparticles decay via gauginos or sleptons. In a search it is not necessary to distinguish between the various contributions to new physics and so both classes of event form part of the signal. However in this study we are particularly interested in the scenario in which all strongly interacting particles are heavy, since in those cases other analyses (requiring jets) will have more difficulty making a discovery. Since we want to be sensitive to SUSY even in this harder case, we define the signal in two different ways:

- "Inclusive SUSY" : Inclusive supersymmetric particle pair production (any sparticles)
- "Direct gaugino" : Direct production of charginos and neutralinos only

[2)] The masses and branching ratios were calculated using Isajet v7.71 [4] using a top mass of 175 GeV.

Table 5: Selection criteria for muons, electrons and jets.

	Muon	Electron	Jet
p_{T} cut	> 10 GeV	> 10 GeV	> 10 GeV
η cut	$\lvert\eta\rvert < 2.5$	$\lvert\eta\rvert < 1.37$ or $1.52 < \lvert\eta\rvert < 2.5$	$\lvert\eta\rvert < 2.5$
Calorimeter Isolation	$\lvert E\rvert < 10$ GeV in $\Delta R = 0.2$	$\lvert E\rvert < 10$ GeV in $\Delta R = 0.2$	- -

Inclusive SUSY represents the signal we would obtain at the benchmark points. Direct gaugino represents a more pessimistic scenario, where coloured sparticles are heavy so have no significant LHC cross-section.

2 Lepton selection

The final selection will require three leptons – electrons or muons – which must consist of an OSSF pair and a further third lepton. The initial lepton selection requirements are based on the ATLAS standard criteria. The main definitions are summarised in Table 5, and are briefly discussed below. The relatively low p_{T} threshold for electrons and muons of 10 GeV in these analyses is an attempt to increase the number of trilepton events, despite lower lepton reconstruction efficiencies at low p_{T} .

- **Muons** must satisfy $p_{\mathrm{T}} > 10$ GeV and $|\eta| < 2.5$, and tracks found in the muon spectrometer must match inner detector tracks. For each muon spectrometer track only the best matching track in the inner detector is taken. It is required that the χ^2 for the match of the muon track to the points on the track [5] is less than 100. A primary isolation criterion requires less than 10 GeV of transverse energy[3)] in the calorimeter in a cone of radius $\Delta R = 0.2$ around the muon[4)].

- **Electrons** must satisfy $p_{\mathrm{T}} > 10$ GeV and $|\eta| < 2.5$. They must satisfy shower shape and isolation requirements as described in [6]. The entire event is rejected if any electron candidate is found in the barrel-endcap transition region ($1.37 < |\eta| < 1.52$) due to the lower electron identification performance in this region. A primary isolation criterion is that electrons must have less than 10 GeV of transverse energy in an annulus of radius ΔR=0.2 surrounding the electron.

Electrons and muons are then subject to further vetoes as follows: electrons and muons within $\Delta R < 0.4$ of a jet are removed from the event, along with OSSF pairs with invariant mass $M_{OSSF} < 20$ GeV, which are likely to have been produced from photon conversions or hadronic decays.

2.1 Single lepton selection efficiencies

Searches for SUSY final states with three leptons require both a high lepton reconstruction efficiency and low fake rates. There are few Standard Model processes with similar signatures, but the high cross section backgrounds $t\bar{t}$ and Zb can pass the trilepton requirement as there are both primary leptons in the event and a number of jets, in particular b jets which can introduce secondary leptons. Good isolation criteria are therefore important in order to reduce the fake rate and thus the background. This section

[3)] Transverse energy, $E_T = E \sin\theta$, where E is the energy and θ is the polar angle relative to the beam direction.

[4)] $\Delta R \equiv \sqrt{\Delta\eta^2 + \Delta\phi^2}$ where $\Delta\eta$ is the pseudorapidity difference, with $\eta \equiv -\log\tan(\theta/2)$, and $\Delta\phi$ is the difference in azimuthal angle.

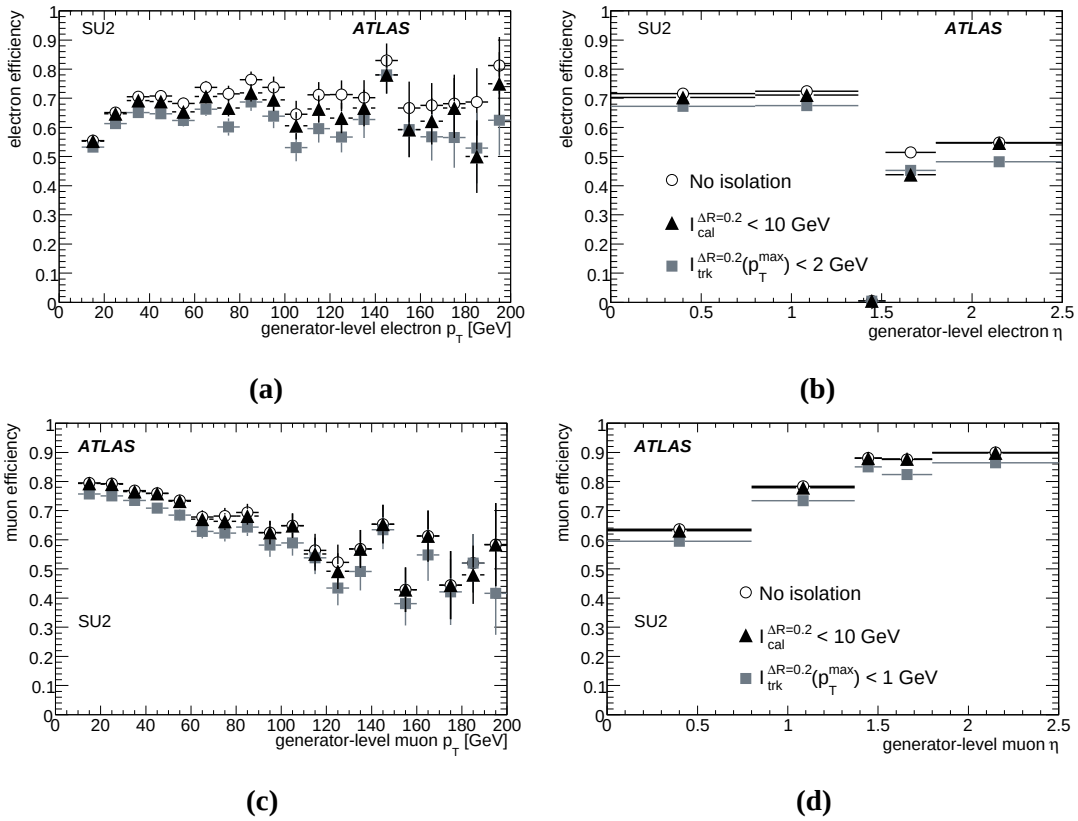

Figure 2: The efficiency for electrons (a,b) and muons (c,d) to be reconstructed and to pass various isolation criteria, for the SU2 sample. The plots are shown as a function of the p_T (a,c) and η (b,d) of the matched Monte Carlo lepton.

presents a study of the lepton efficiency, fake rate and purity for the common object definition which includes a calorimeter based isolation criterion as well as the performance of a track-based alternative.

When collision data are available, the best determination of these quantities will be made from the ATLAS data using the methods described in [7]. Since most of our events of interest will have a similar environment – isolated leptons and little jet activity – we may expect that the values found in those studies should closely match the corresponding quantities in our search. However since those measurements require collision data, in this section we present the efficiencies, fake rates and purities as determined from Monte Carlo information only.

The following isolation criteria have been studied:

- **No isolation cut** - showed as a reference;
- **Calorimeter-based isolation** $E_{\text{cal}}^{\Delta R=0.2} < 10$ GeV. $E_{\text{cal}}^{\Delta R=0.2}$ is the energy deposited in a cone with $\Delta R = 0.2$ around the lepton candidate;
- **Maximum-p_{T} track-based isolation** $p_{T\,\text{track,max}}^{\Delta R=0.2}(\ell) < 2/1\,\text{GeV}$ for e/μ, where $p_{T\,\text{track,max}}^{\Delta R=0.2}(\ell)$ is the maximum p_T of any track in a $\Delta R = 0.2$ cone around the lepton;
- **Sum-p_{T} track-based isolation** $p_{T\,\text{track},\Sigma}^{\Delta R=0.3}(\ell) < 4\,\text{GeV}$, where $p_{T\,\text{track},\Sigma}^{\Delta R=0.3}$ is the sum of the p_{T} of all tracks above 1 GeV in a $\Delta R = 0.3$ cone around the lepton.

The lepton reconstruction efficiency is defined to be

$$\mathscr{E}_\ell \equiv \frac{n_\ell^{\text{match}}}{n_\ell^{\text{MC}}} \ , \tag{1}$$

where n_ℓ^{match} is the number of *generator-level* leptons matched to a reconstructed candidate and n_ℓ^{MC} is the total number of generator-level leptons.

In this study generator-level leptons are defined to be charged leptons ($\ell \in \{e, \mu\}$) which have come from decays of SUSY particles (sleptons and gauginos), Standard Model gauge bosons and tau leptons, but do *not* include leptons from other sources (such as hadronic decays, bremsstrahlung, or photon conversions). No isolation cut has been applied on these generator-level leptons. Generator-level particles are matched to reconstructed candidates which have passed kinematics cuts and object selection according to the definition in Section 2. A match is required to be found within $\Delta R = 0.02$. Figure 2 shows the reconstruction efficiency for electrons and muons from the SU2 sample using different isolation requirements as function of the p_{T} and η of the matched Monte Carlo lepton.

The requirement that leptons should be separated from selected jets by $\Delta R > 0.4$ (referred to as the $\Delta R(\ell, \text{jet}) > 0.4$ cut) is already a strong isolation requirement which reduces the efficiency by $\sim 5\%$ for electrons and $\sim 15\%$ for muons. For the case of $t\bar{t}$ events (not shown in the figures) the effect is even larger as there are more jets in the events.

For the muons, one can see that after introducing the $\Delta R(\ell, \text{jet}) > 0.4$ cut, the efficiency decreases with increasing p_T , while the $|\eta|$ distribution decreases in the central region $|\eta| \lesssim 1.4$. A clear drop in electron efficiency can be found near $|\eta| \approx 1.4$ which is the barrel-endcap transition region.

After applying only the $\Delta R(\ell, \text{jet}) > 0.4$ cut (referred to as "no isolation" in the plots), the total efficiency is $(65.5 \pm 0.5)\%$ and $(75.2 \pm 0.5)\%$ for electrons and muons respectively. The calorimeter-based isolation $E_{\text{cal}}^{\Delta R=0.2} < 10\,\text{GeV}$ reduces the electron efficiency by $\approx 3\%$ to $(63.6 \pm 0.5)\%$ while leaving the muon efficiency almost unchanged. The track-based alternative has similar effect on both lepton flavours causing a loss of about 7 to 8% with respect to the "no isolation" performance.

The fake rate is defined as

$$\mathscr{F}_\ell \equiv \frac{n_\ell^{\text{MC},\overline{\text{match}}}}{n_{\text{jet}}^{\text{MC}}} \ , \tag{2}$$

where $n_\ell^{\text{MC},\overline{\text{match}}}$ is the number of reconstructed leptons which are *not* matched to a generator-level lepton and $n_{\text{jet}}^{\text{MC}}$ is the number of jets at the generator level[5)].

Only generator-level jets with $|\eta| < 2.5$ are considered. They are rejected if there is an overlap with an electrons within $\Delta R < 0.2$, but in general include photons, hadronic tau jets and b jets. The generator jet must have energy, $E > 7$ GeV. Asymmetric p_{T} cuts are applied to the reconstructed objects compared to their Monte Carlo equivalents. For the efficiency calculation $p_{\text{T}\ell}^{\text{MC}} > 10$ compared to $p_{\text{T}\ell} > 5$ GeV, while for the fake rate calculation $p_{\text{T}}{}^{MC} > 5$ and $p_{\text{T}\ell} > 10$ GeV. This reduces the number of mismatches which would be found near the edge of the fiducial region from small mismeasurements of p_{T} .

Figure 3 shows the fake rate as function of the p_T and η of the fake lepton for the $t\bar{t}$ sample (one of the major backgrounds). The p_{T} distribution is clearly peaked at low values typical for leptons from b-jet decays. The η distribution follows the detector layout with higher fake rate in the transition region between the barrel and end caps.

The $\Delta R(\ell, \text{jet}) > 0.4$ requirement provides a reduction in the fake rate of about $\approx 80\%$ for muons and $\approx 5\%$ for electrons (as compared to leptons passing the standard selection with $E_{\text{cal}}^{\Delta R=0.2} < 10$). With no isolation other than the $\Delta R(\mu, \text{jet}) > 0.4$ requirement one obtains a fake rate of $(4.1 \pm 0.1) \times 10^{-3}$ and $(1.1 \pm 0.1) \times 10^{-3}$ for electrons and muons respectively. The isolation criteria provide a similar relative

[5)] *i.e.* jets found by running a jet algorithm over the Monte Carlo generator final state, before detector simulation.

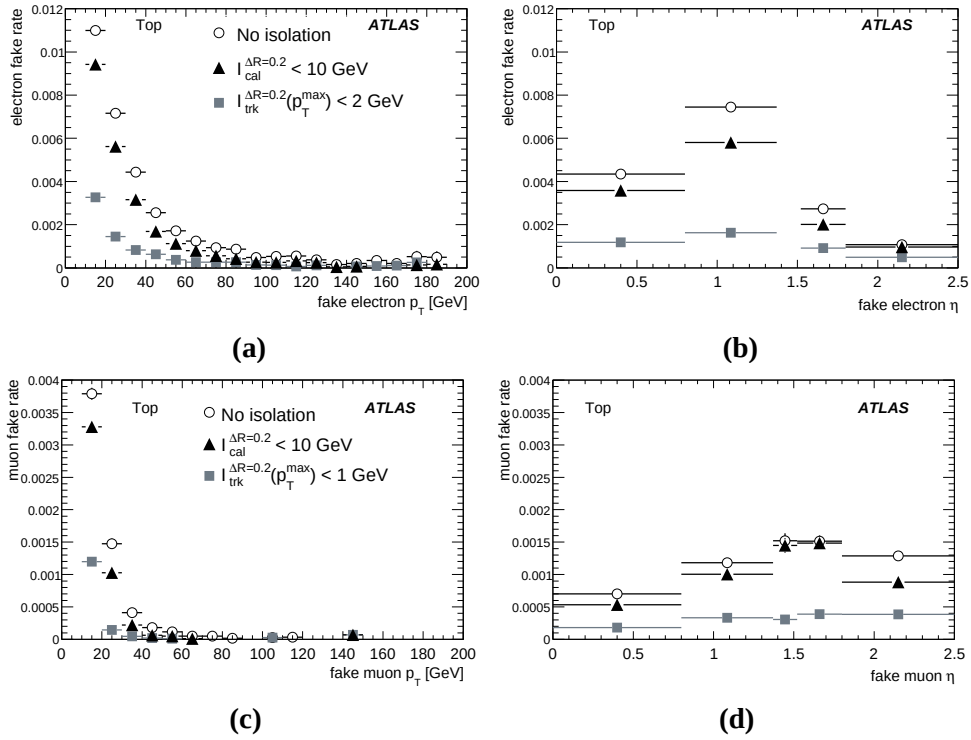

Figure 3: The fake rate for electrons (a,b) and muons (c,d) in the $t\bar{t}$ sample as function of the p_T (a,c) and η (b,d) of the fake lepton.

suppression of the electron and muon fake: $\approx 20\%$ for $I_{\text{cal}}^{\Delta R=0.2} < 10$ and $\approx 74\%$ for $p_{T\text{track,max}}^{\Delta R=0.2}(\ell) < 2/1\,\text{GeV}$ for e/μ. The effect of the isolation cuts is very similar in the case of the SU2 sample, but the fake rates are almost an order of magnitude lower than in $t\bar{t}$ events.

We define purity by:

$$\mathscr{P}_\ell = \frac{n_\ell^{\text{match}}}{n_\ell} \,, \tag{3}$$

where n_ℓ is the number of reconstructed leptons, and the matching criteria are as described above. The lepton selection described in Section 2 provide samples with a purity of 92% (e) and 97% (μ) with very similar results for both the SU2 and $t\bar{t}$ samples. However after requiring at least 3 leptons in the event there is a clear difference between the two. The purity is almost unchanged for SU2, while, in $t\bar{t}$ trilepton events the purity drops to $\sim 50\%$ for electrons and $\sim 70\%$ for muons.

3 Event selection

Events are required to pass either of the two single-lepton triggers, labelled L2_e22i and L2_mu20, which are well-suited for the tri-lepton analysis at $\mathscr{L} = 10^{31-32}\,\text{cm}^{-2}\text{s}^{-1}$. A more detailed discussion of the motivation for using these triggers can be found in Section 5.

Distributions of some important event variables for Standard Model backgrounds and for the benchmark point SU2 (both for inclusive SUSY and direct gaugino) can be found in Figure 4. We show the p_{T} distributions of reconstructed leptons (electron or muon) and jets. Requiring at least three leptons in the event results in mainly $t\bar{t}$ and Zb Standard Model backgrounds, with larger contributions from dibosons in four lepton events. It can seen in Figures 4a and 4b that p_{T} distributions of the two hardest leptons

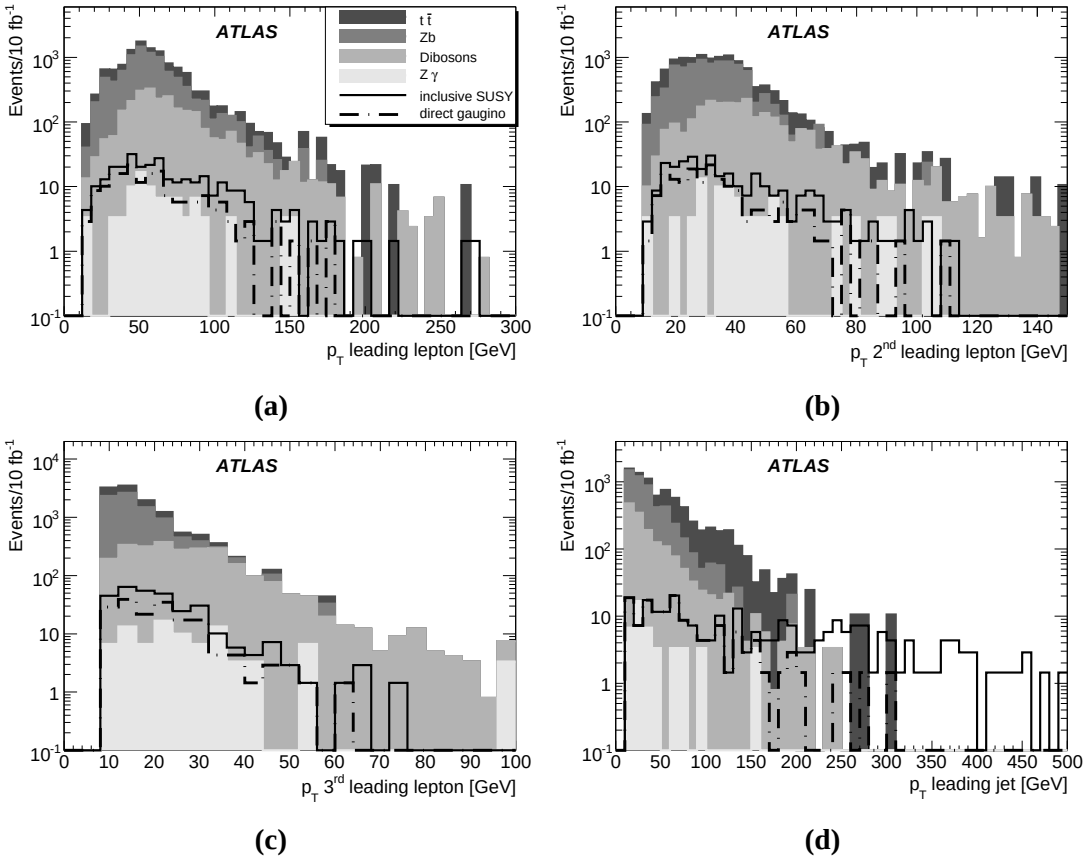

Figure 4: Transverse momentum of the leading three leptons (a-c) and leading-jet p_{T} (d) after an initial three-lepton requirement has made.

in three lepton events are similar in SU2 and $t\bar{t}$, with Zb adding a significant contribution in the low p_{T} region. The p_{T} distributions for the third-hardest leptons are plotted in Figure 4c where it can be seen that whilst $t\bar{t}$ and Zb are the major backgrounds in the low p_{T} region, there is a large contribution from the dibosons across the entire p_{T} range. This is because the third leptons from $t\bar{t}$ and Zb are soft leptons from leptonic b-quark decay, whereas all the leptons from dibosons are from $Z/W^{\pm}$ boson decays. The p_{T} distributions of the reconstructed jets are plotted in Figure 4d for events with three or more leptons.

Since an OSSF lepton pair is expected from the $\tilde{\chi}_2^0$ decay, a selection requiring two OSSF leptons is applied (i.e. we require $e^+e^- + \ell$ or $\mu^+\mu^- + \ell$, where $\ell \in e, \mu$)[6]. A further cut requires three or more leptons in the event.

A stringent cut on the isolation of the tracks of the leptons is made next, using the $p_{T\,\mathrm{track,max}}^{\Delta R=0.2}$ variable described in Section 2.1. The purpose is to reduce backgrounds from bremsstrahlung, hadron decays and photon conversions. The relevant distributions for electrons and muons are plotted in Figure 5a and 5b. The plots contain negative entries when no track is found within ΔR. We require $p_{T\,\mathrm{track,max}}^{\Delta R=0.2} < 1$ GeV for muons and < 2 GeV for electrons. This reduces the number of background events to 23% ($t\bar{t}$) and 37% (Zb) of their previous levels, whilst keeping 82% (inclusive SUSY), 86% (direct gaugino) of the signal for our SU2 benchmark point.

[6] Trilepton events where all three leptons have the Same Sign, (SS, $\ell^{\pm}\ell^{\pm}\ell^{\pm}$, where $\ell \in e, \mu$) have also been investigated, however due to the very low statistics associated with the channel in the signal samples investigated, it is not considered further here.

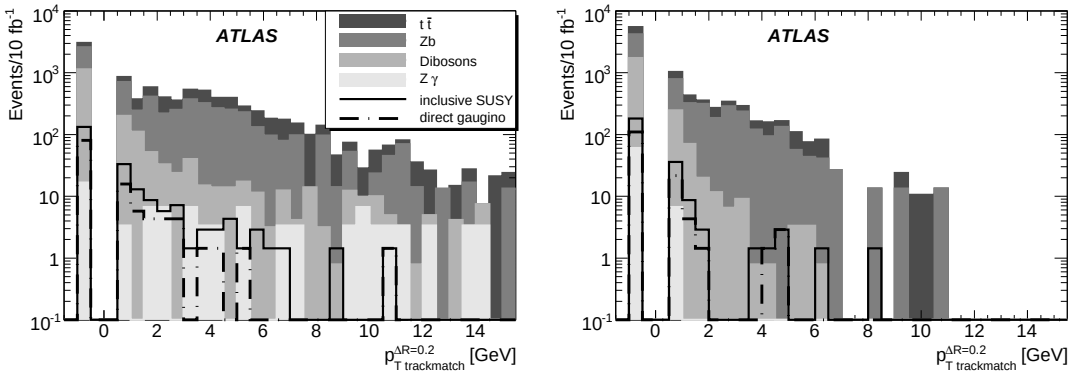

(a) **(b)**

Figure 5: $p_{T\,\mathrm{track,max}}^{\Delta R=0.2}$ for **(a)** electrons and **(b)** muons.

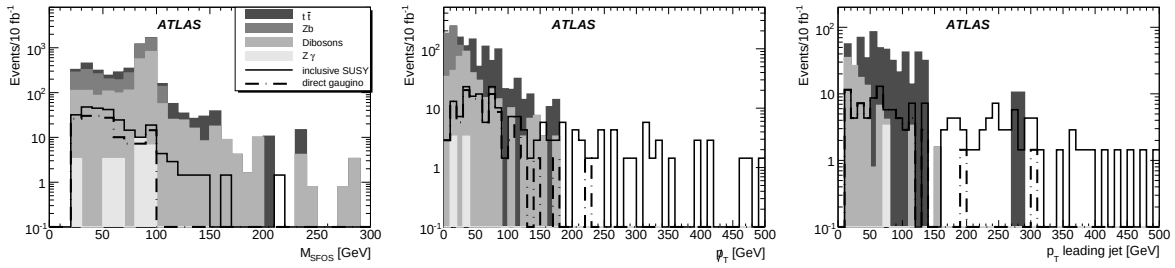

(a) **(b)** **(c)**

Figure 6: **(a)** OSSF dilepton invariant mass distribution. **(b)** $E_{\mathrm{T}}^{\mathrm{miss}}$ distribution after the Z mass window cut. **(c)** The p_{T} distribution of the leading jet after the $E_{\mathrm{T}}^{\mathrm{miss}}$ cut is applied.

The diboson and Zb backgrounds will produce the two OSSF leptons mainly from Z decays, which will not be the case for three-body decays of neutralinos. The dilepton invariant mass distribution is shown in Figure 6a, (after applying the cuts already described) and shows the expected peak at the Z mass. A simple way to reduce the these backgrounds is to discard events which have any OSSF dilepton pair with invariant mass in the mass window 81.2 GeV $< M_{OSSF} <$ 101.2 GeV. Note that this exclusion window also offers an excellent control region in which to measure the size of these backgrounds from the data. It is however somewhat model-dependent. Some points in SUSY parameter space preferentially decay through *real Z* bosons, rather than through three-body decays. At those points the OSSF dilepton mass distribution would also be strongly peaked at the Z mass.

A large missing-transverse-momentum cut is used in most SUSY analyses, but in this analysis a smaller cut at 30 GeV is applied since in direct gaugino production the two invisible $\tilde{\chi}_1^0$s are often almost back-to-back in the transverse plane, resulting in a lower overall $E_{\mathrm{T}}^{\mathrm{miss}}$ (Figure 6b). Missing transverse momentum is calculated as described in [8].

Finally there is the possibility of adding a cut can be made on the hadronic activity in the event. This could be useful in the case where direct gaugino production dominates, since it can be expected to reduce the $t\bar{t}$ background to a greater extent than the signal. Whether this cut is appropriate will depend on the SUSY scenario presented by nature, so analyses both with and without this cut will be necessary.

Selected jets must satisfy $p_{\mathrm{T}} > 10$ GeV and $|\eta| < 2.5$, and are reconstructed based on calorimeter tower signals [9] using a seeded cone algorithm with radius $\Delta R = 0.4$. Jets are initially selected with

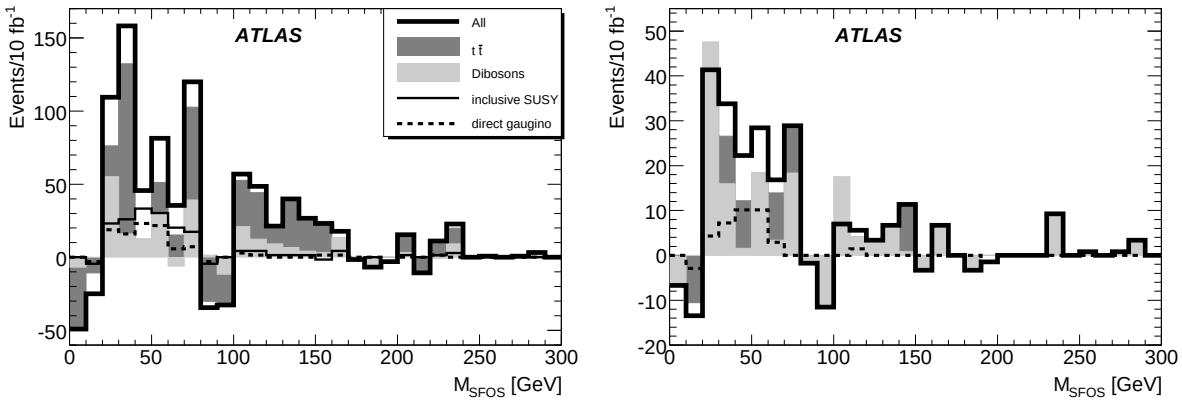

(a) **(b)**

Figure 7: Distributions of the OSSF dilepton invariant mass after all selections have been applied **(a)** without the jet veto and **(b)** including a jet veto.

$p_{\mathrm{T}} > 10$ GeV and $|\eta| < 2.5$. Jets are not considered if they overlap with a reconstructed electron within $\Delta R < 0.2$.

The p_{T} distribution of the leading jet in the event is plotted in Figure 6c, where it is seen that the direct gaugino production has jets with lower p_{T} than the Standard Model backgrounds. The level of this cut is chosen at $p_{\mathrm{T}} > 20$ GeV.

The complete event selection is then:

1. At least one pair of OSSF leptons (e^+e^- or $\mu^+\mu^-$)
2. $N_\ell >= 3$ ($\ell \in \{\mathrm{e}, \mu\}$), and where all ℓ_i satisfy the requirements in Section 2
3. $p_{T\,\mathrm{track,max}}^{\Delta R=0.2} < 2$ GeV for electrons, $p_{T\,\mathrm{track,max}}^{\Delta R=0.2} < 1$ GeV for muons
4. No OSSF dilepton pair has invarint mass in the range 81.2 GeV $< M_{OSSF} <$ 102.2 GeV
5. $E_{\mathrm{T}}^{\mathrm{miss}} > 30$ GeV
6. Optional – no jet with $p_{\mathrm{T}} > 20$ GeV

In Figure 7 we show distributions of the invariant mass of the dilepton pair after all cuts. The distributions have been flavour subtracted; the quantity plotted is

$$n^{\mathrm{OSSF}} - n^{\overline{\mathrm{OSSF}}}, \tag{4}$$

where n^{OSSF} is the number of events in the signal selection (containing OSSF dilepton pairs) as described earlier in this section, and $n^{\overline{\mathrm{OSSF}}}$ is the number of events in which there are three leptons, but no OSSF pair. The non-OSSF events give an indication of the expected background size since many background sources do not necessarily produce OSSF pairs.

4 Discovery potential

The numbers of events and the resulting significance at each stage of the analysis are listed in Table 6 for the benchmark point SU2. We use the following definition of signal signficance,

$$\mathscr{S} = \frac{S}{\sqrt{S+B}} \tag{5}$$

where S is the number of signal events and B is the number of background events. After applying the event selection above (including the jet veto), 29 events remain for SU2 inclusive SUSY all of which are direct gaugino, with an expected background of 210 events (mainly ZW production). This corresponds to $\mathscr{S}$ of 1.87 for 10 fb^{-1} . This yields a 5σ discovery signal after $\sim$80 fb^{-1} of integrated luminsity. With the jet veto selection, ZW is the dominant remaining Standard Model background. Without the jet veto, 177 signal events (95 of them direct gaugino) remain. Statistical significances of 5.94 and 3.34 are found for the inclusive SUSY and direct gaugino signals respectively.

Table 6: Numbers of events and statistical significance as selection is applied for the benchmark point SU2, for integrated luminosity of 10 fb^{-1}.

Kinematic Cut	No Cuts	$N_L >= 2$	OSSF	$N_L >= 3$	TrackIsol	$m_{\ell\ell}$	$E_{\mathrm{T}}^{\mathrm{miss}}$	JetVeto
SU2 gauginos	64.0k	1647	1108	178	153	120	95	29
SU2 other	7081	776	353	127	95	85	82	0
$t\bar{t}$	4.41M	234k	104k	2812	634	507	476	42
ZZ	38.2k	10.4k	9984	580	476	57	13	6
ZW	156k	17.2k	14.5k	1910	1682	322	218	154
WW	400k	22.7k	10.7k	25	8	8	8	8
$Z\gamma$	32.8k	7184	6970	91	27	7	3	0
Zb	1.59M	57.4k	559k	6523	2409	386	0	0
inclusive SUSY $\mathscr{S}$		2.60	1.74	2.76	3.36	5.31	**5.94**	**1.87**
direct gaugino $\mathscr{S}$		1.77	1.32	1.61	2.09	3.20	**3.34**	**1.87**

The expected statistical significances for various mSUGRA benchmark points are summarised in Table 7 excluding the jet veto unless indicated otherwise by "SUx+JV".

Table 7: Discovery potential, and integrated luminosity required for 5σ discovery. The jet veto is only applied in columns headed '+JV'. For a fuller description of the notation, see the text.

	SU1	SU2	SU3	SU4	SU8	SU2χ	SU3χ	SU2+JV	SU3+JV
$\mathscr{S}$, 10 fb^{-1}	7.7	5.9	17.2	69.3	1.9	3.3	1.6	1.9	1.4
$\int$d$t\,\mathscr{L}$ for 5σ	4.2	7.1	0.8	0.1	70.5	22.4	92.9	66.9	119.3

The discovery prospects for inclusive SUSY, reflected in columns titled "SUx", are rather encouraging: a 5σ discovery can be expected with several fb^{-1} of integrated luminosity[7)]. The direct gaugino pair production is highlighted in columns marked as SU2χ and SU3χ. Both for SU2 and SU3 we see a drop in significance which roughly corresponds to the fraction of the direct gaugino production compared to the total SUSY cross-section. In fact, the drop is somewhat higher, since the p_{T} spectrum tends to be softer for direct gaugino pair production compared to strong SUSY production with its characteristic decay chains. Here, a discovery can be expected with several tens of fb^{-1}.

[7)] Taking into account statistical errors only. Systematic uncertainties are discussed in Section 6.5.

Table 8: Fraction of events triggered at L2 at three selection stages of the selection for the heavy coloured sparton scenario in SU2 (first block), the direct gaugino production in SU3 (second block), and the inclusive SU3 signal (third block). "$\bigcup$" stands for the OR-combination of L2_e22i and L2_mu20.

Selection	SU2χ			SU3χ			SU3 incl.		
Stage	L2_e22i	L2_mu20	$\bigcup$	L2_e22i	L2_mu20	$\bigcup$	L2_e22i	L2_mu20	$\bigcup$
OSSF pair	41%	54%	89%	42%	54%	92%	51%	51%	94%
OSSF+3$^{\text{rd}}\ell$	58%	67%	93%	59%	63%	95%	66%	68%	98%
after all cuts	57%	66%	92%	58%	57%	94%	66%	64%	97%

5 Lepton trigger study

Unlike most SUSY searches, in this channel we cannot rely on jet or $E_{\text{T}}^{\text{miss}}$ triggers. We have studied a variety of triggers at the second level[8], after the first level trigger has been applied. Other studies [10,11] demonstrate that objects passing L2 have a high efficiency for passing EF.

As a figure of merit, the fractions of triggered events

- after selecting for an OSSF pair;
- after requiring a further third lepton;
- after all cuts, including the jet veto;

are studied.

We have identified two single-lepton triggers, labelled L2_e22i and L2_mu20, that are well-suited for the tri-lepton analysis at $\mathscr{L} = 10^{31-32}\,\text{cm}^{-2}\text{s}^{-1}$. At high luminosity it is planned to have corresponding triggers with additional isolation criteria (e22i_tight and mu20i) which will remain unprescaled. The resulting event-triggering efficiencies are listed in Table 8. OR-combined, they have ≈92% probability for direct gaugino production for the benchmark point SU2. They have sufficiently high p_T thresholds to be easily studied with leptonic Z decays.

The same trigger set was studied for the direct gaugino and inclusive SUSY for another bechmark point, SU3, that has lighter squarks than SU2. Again the OR-combination of L2_e22i and L2_mu20 shows a good performance of $\sim$92, 95, 94%. Their individual L2 event efficiencies are summarised in the middle block of Table 8.

In addition we have studied the performance of the L2_e22i and L2_mu20 triggers for the tri-lepton analysis, outside of the heavy coloured sparton scenario, for inclusive SU3 production. Again in this case we find L2 event efficiencies of around $\sim$94, 98, 97%.

The efficiency is relatively high for lepton triggers even though the trigger thresholds are fairly high compared to the offline cuts on lepton transverse momenta. The reason for that is simple combinatorics: since the 3 leptons are ordered by their transverse momenta, it is likely that the leading lepton has a high p_T if the third one passes the offline threshold. On the other hand, cases where *all* the three leptons are below $20-30$ GeV but above 10 GeV are unlikely.

We have investigated how the leptonic trigger efficiencies for the inclusive SUSY and direct gaugino for the benchmark point SU2 change as a function of the progressive event selection stages described in Section 3. In both cases, the trigger efficiencies reach their approximate maxima after the three-lepton selection stage. Beyond this cut stage, the efficiency values plateau, indicating that our event

[8] ATLAS has three trigger levels: a first level (L1) hardware trigger, a software-based second level trigger (L2) that examines regions of interest within the decector, and finally a software-based event filter (EF). More details about the electromagnetic [10] and muon [11] triggers may be found elsewhere in this volume.

selection requirements should not bias signal trigger efficiencies. It can be concluded that the L2_e22i and L2_mu20 single lepton triggers provide a good performance for the tri-lepton analysis in the early days of ATLAS running at $\mathscr{L} = 10^{31}\,\mathrm{cm}^{-2}\mathrm{s}^{-1}$. Di-leptonic triggers with lower thresholds like 2e12i, 2mu10, and e15i_mu10 can be used to recover events where all three leptons have low transverse momenta around 20 GeV.

6 Systematic uncertainties

The dominant sources of systematic uncertainty for this search are different to other SUSY search channels that focus on final states containing jets. For our multi-lepton search the main sources of uncertainty in the backgrounds are described below.

6.1 Background rates

The production rates for the majority of background processes such as diboson production and $t\bar{t}$ are known at the parton level at better than next-to-leading order. However, it is generally better to determine the rate of these backgrounds from the ATLAS data themselves, reducing any uncertainty from luminosity, PDFs and other systematics (e.g. from acceptances, efficiencies etc). The background rate measurements should be made in "control regions" in which they dominate. For the WZ background a sensible control region is the region of phase space where the OSSF lepton pair has an invariant mass near the m_Z [12]. For the $t\bar{t}$ background, one would examine single lepton and OSSF dilepton channels [13]. Any statistical uncertainty in the background measurements forms a systematic uncertainty in our analysis. The expected integrated luminosities for cleanly measuring each background and the resulting statistical uncertainties can be found in Table 9.

Any further systematic uncertainties in the background rates are not considered here so as not to double-counting their effects[9)]. One must be careful that the extrapolation from the 'control' to the 'measurement' region of parameter space is well understood. The extrapolation for the backgrounds involving the Z peak relies on the Z line-shape, which is theoretically well-known. The extrapolation from dilepton to trilepton final states for $t\bar{t}$ relies on a good knowledge of the rate at which b quarks (from top decays) produce isolated leptons. A method of determining this rate from the ATLAS data is presented in Section 6.3.

Table 9: Expected rates to cleanly select background samples in control regions, and the corresponding statistical uncertainties.

Background	Statistical uncertainty after 10 fb^{-1} [%]	Reference
WW	1.3	[12]
WZ	2.6	[12]
ZZ	6.6	[12]
$t\bar{t}$	$\ll 1$	[13]

One can see from Table 6 that, after event selection and jet veto, the WZ and $t\bar{t}$ backgrounds are most significant in the signal region. The systematic uncertainty in measuring the rate of the backgrounds in

[9)] In fact, uncertainties on background rates that positively correlate between the selection region and the control region will actually tend to cancel.

the control regions is expected to be of the order of a few percent maximum for the WZ and even smaller for the $t\bar{t}$ (Table 9). Our estimate for the total systematic uncertainty due to statistical fluctuations in the background control sample is therefore dominated by the WZ background. When multiplied by the fraction of the final background that comes from WZ, this generates 1.9% (0.8%) uncertainty in the background rate for the analysis with (without) the jet veto.

6.2 Trigger and reconstruction efficiencies

Lepton trigger and reconstruction efficiencies can be determined using the "tag-and-probe" method for electrons and muons coming from $Z \to \ell\ell$ [7].

Table 10: Expected systematic uncertainties on background rates from other ATLAS measurements using the tag-and-probe method, and resultant estimated uncertainties for this analysis. The label 'reco' refers to combined reconstruction and selection efficiencies.

Source	Tag-and-probe [7] ($1\ell^{\pm}$, 1fb^{-1})	This analysis (10 fb^{-1}) $1\ell^{\pm}$	This analysis (10 fb^{-1}) $3\ell^{\pm}$
e (trigger)	$\ll 1\%$	$\}$ 0.5 %	$\Big\}$ 2.3%
μ (trigger)	0.4 %		
e (reco)	0.5 %	1 %	
μ (reco)	$\ll 1\%$	$\ll 1\%$	

The precision with which lepton trigger and reconstruction efficiency can be determined has been studied in [7] for an integrated luminosity scaled to 1 fb^{-1}. The statistical uncertainty on the trigger efficiency for 1 fb^{-1} is very small ($\ll 1\%$) and is negligible for 10 fb^{-1}. The systematic uncertainties in determining the trigger efficiencies are shown in Table 10. The trigger efficiency uncertainty for our analysis, for which the highest-p_{T} lepton has similar kinematics to the sample used in [7], is therefore estimated to be $\lesssim 0.5\%$ for $\int \mathrm{d}t\,\mathscr{L} = 10$ fb^{-1}.

Reconstruction and selection efficiencies have also been studied using a similar method [7]. The estimates of the uncertainties in the efficiencies are also contained in Table 10. We have increased the expected uncertainty in the electron reconstruction efficiency from the "tag-and-probe" value of 0.5% to our own estimate of 1% to reflect a somewhat larger uncertainty for our lower p_{T} electrons.

In the final column of Table 10 we estimate the resulting systematic uncertainty for the trilepton selection efficiency of this analysis. Since we propose using single lepton triggers (Section 5), only the highest p_{T} lepton contributes, and our event trigger uncertainties are the same as the single-lepton trigger ones. All three leptons are assumed to contribute to reconstruction and selection uncertainties, with equal contributions from electrons and muons. Our resulting uncertainty from combined trigger, reconstruction and selection efficiencies is 2.3%.

For this study we assume that similar uncertainties will apply with and without the jet veto, but we note that there may be larger systematic uncertainties in lepton efficiencies if jets are permitted in the final state.

6.3 Lepton fake rates

The $t\bar{t}$ and $Z+b$ backgrounds contribute to the trilepton final state when (along with a lepton pair from dileptonic $t\bar{t}$ decay or Z decay) a B hadron decays leptonically, producing a third isolated lepton. The third lepton requirement reduces each of these backgrounds by a large factor – about two orders of magnitude in each case. About one order of magnitude of reduction can be accounted for by the

branching ratio of B hadrons to leptons, while the other factor of about ten arises from our rejection of non-isolated leptons. We are therefore sensitive to the rate at which leptons from b decays pass the isolation criteria, which we denote $R_{b\to\ell}$ (it should be understood to include leptons both from direct $b\to\ell$ and also from $b\to c\to\ell$).

We hereby propose a method by which $R_{b\to\ell}$ could be measured in the ATLAS data, and estimate the remaining systematic uncertainty after that measurement. The control sample we suggest is semi-leptonic $t\bar{t}$ decays in which a lepton from one (probe) b decay generates a same-sign dilepton pair. To cleanly select the control sample we would require events with $t\bar{t}$ kinematics (*e.g.* consistent invariant masses for t and W) and one clean vertex tag from the other (probe) b jet. This sample has the further advantage that the b quarks have the correct kinematical distributions for the background of interest (dileptonic $t\bar{t}$). The same-sign dilepton requirement removes contamination from normal dileptonic $t\bar{t}$ decays since the latter will produce opposite-sign lepton pairs.

Dedicated studies [13] suggest that we can expect to cleanly select about $n_{t\bar{t}->\ell} = 5\times10^4$ semi-leptonic $t\bar{t}$ events (e and μ combined) for $\int \mathrm{d}t\,\mathscr{L}$=10 fb^{-1}. The fractional statistical uncertainty, δ, that we could expect from the proposed measurement of $R_{b\to\ell}$ is then,

$$\delta(R_{b\to\ell}) = \frac{1}{\sqrt{R_{b\to\ell}\times n_{t\bar{t}->\ell}}}\ . \tag{6}$$

From examination of the event record in our Monte Carlo samples, we found $R_{b\to\ell}$ to be approximately 5×10^{-3}. If a similar rate were to be found from measurements of the semi-leptonic $t\bar{t}$ events, then the corresponding value for $\delta(R_{b\to\ell})$ would be 6%.

With a jet veto, $t\bar{t}$ forms about 20% of the background after full selection (and $Z+b$ a very small contribution), and there is a resulting $\approx 1.2\%$ uncertainty in the total background. Without the jet veto, the $t\bar{t}$ contribution is much larger (about 66%) and a 4% systematic uncertainty results.

6.4 Jet and missing energy scales

The global uncertainty on the jet energy scale is currently conservatively expected to be about 5%, but the true value is difficult to determine without collision data. In events in which the missing transverse momentum is dominated by hadronic activity, the fractional uncertainty in $E_{\mathrm{T}}^{\mathrm{miss}}$ will be of a similar size, since the two measurements will be highly correlated. We therefore determined the effect of a 5% systematic uncertainty in the missing energy when no jet veto is used.

For the analysis which includes a jet veto, we expect missing energy scale uncertainty to be rather smaller than 5%, since the majority of the missing energy will recoil against the (well-measured) leptons. We also assume that in this case the systematic uncertainties in the jet energy scale and the missing energy should also be largely uncorrelated (for the same reason). Measurements of recoil of jets against Z bosons and photons allow the missing energy resolution to be well-determined as a function of jet energy [8]. Any residual uncertainty in the missing energy scale is estimated by us to be about 2% at low hadronic energies (based on systematic differences between methods in [8]).

For the jet-veto analysis, we determined the effects of a 5% variation in the hadronic energy scale and (an independent) 2% variation in the missing energy scale. The results are shown along with the systematic uncertainties from other sources in Table 11.

As well as the uncertainty from the energy scales, there can be some contribution to the uncertainty in the number of events failing the jet veto from our lack of knowledge of initial-state radiation (ISR) in electro-weak processes (such as WZ production). However the ISR spectrum can be readily determined from other electroweak production control regions (as described in [14] for single electroweak gauge boson production). The resulting statistical uncertainties in those control measurements will be small, and the systematic effects tend to cancel with those described in this section, so no additional systematic uncertainty is added here.

6.5 Summary of systematic uncertainties

Table 11: Estimates of the dominant uncertainties in the background determination for $\int dt\,\mathscr{L} = 10$ fb^{-1}.

Source	Uncertainty	
	No jet veto	With jet veto
Background production rates	0.8%	1.9%
Lepton Efficiency	2.3%	2.3%
Fakes ($R_{b\to\ell}$)	4.0%	1.2%
Hadronic energy scale	–	1.8%
Missing energy scale	1.5%	1.0%
Total systematic	4.9%	3.8%
Statistical	3.7%	6.9%
Statistical + Systematic	6.2%	7.9%

Our best current estimates of the various sources of uncertainty are summarised in Table 11. One can see that with the full selection, including the jet veto, and if the supporting measurements can be made with the precision expected, then the SUSY-search analysis will be limited by statistical fluctuations in the background samples (about 6.9%) rather than by systematic sources of uncertainty (about 3.8%).

Without the jet veto, the statistical uncertainty is smaller, however the systematic contribution to the total uncertainty increases to 4.9%, largely because we have an increased sensitivity to $R_{b\to\ell}$ since the top background is much larger if no jet veto is applied.

7 Conclusions

The ATLAS experiment will have sensitivity to new physics, including supersymmetry, in events with three leptons in association with missing transverse momentum. For most of the SUSY benchmark points studied, a discovery of new physics could be made in this channel with integrated luminosity of several fb^{-1} . Models in which all strongly interacting partner particles are heavy would have smaller cross-sections, but could also be discovered with integrated luminosity of the order of several tens of fb^{-1} .

The major sources of systematic uncertainty were indicated and methods for determining these from data discussed. While the actual sizes of these uncertainties can only be estimated reliably with collision data, estimates based on existing information were presented. In particular, knowledge of the rate at which which b jets lead to seemingly-isolated leptons was found to be an important element in understanding Standard Model backgrounds. A method of measuring this rate from the data using $t\bar{t}$ events was proposed.

References

[1] ATLAS Collaboration, *Supersymmetry searches with ATLAS*, this volume.

[2] ATLAS Collaboration, *Prospects for SUSY discovery based on inclusive searches*, this volume.

[3] U. De Sanctis, T. Lari, S. Montesano and C. Troncon, Eur. Phys. J. **C52** (2007) 743–758.

[4] F. Paige, S. Protopopescu, H. Baer and X. Tata, *ISAJET 7.69: A Monte Carlo event generator for p p, anti-p p, and e+ e- reactions* hep-ph/0312045, 2003.

[5] ATLAS Collaboration, *Muon reconstruction and identification performance in ATLAS: studies with simulated Monte Carlo samples*, this volume.

[6] ATLAS Collaboration, *Reconstruction and identification of electrons in ATLAS*, this volume.

[7] ATLAS Collaboration, *Electroweak boson cross-section measurements with ATLAS*, this volume.

[8] ATLAS Collaboration, *Measurement of missing transverse energy in ATLAS*, this volume.

[9] ATLAS Collaboration, *Jet reconstruction performance in the ATLAS detector*, this volume.

[10] ATLAS Collaboration, *Overall trigger strategy for the electron and photon selection*, this volume.

[11] ATLAS Collaboration, *Performance of the ATLAS muon trigger slice with simulated data*, this volume.

[12] ATLAS Collaboration, *Diboson physics studies with the ATLAS detector*, this volume.

[13] ATLAS Collaboration, *Determination of top pair production cross-section in ATLAS*, this volume.

[14] ATLAS Collaboration, *Production of jets in association with W or Z Bosons*, this volume.